

WETTABILITY OF ALUMINIUM WITH SiC AND GRAPHITE IN ALUMINIUM FILTRATION

Sarina Bao¹, Anne Kvithyld², Thorvald Abel Engh¹, Merete Tangstad¹
¹Norwegian University of Science and Technology, Trondheim, NO-7491, Norway
²SINTEF Materials and Chemistry, Trondheim, N-7465, Norway

Keywords: Wettability, Contact angle, Aluminium, Graphite, SiC, Time dependent property

Abstract

The aim of aluminium filtration is to remove inclusions such as Al_3C_4 . For inclusions to be removed they have to come in close contact with the filter walls composed of Al_2O_3 or SiC. It is therefore important that the molten aluminium has close contact with the filter wall. In addition to wetting properties between inclusions (Al_4C_3) and molten aluminium, the wettability of the filter (SiC) by aluminium is determined in sessile drop studies in the temperature range 1000-1300°C. Wettability changes with time in three successive steps and improves with time. To describe wettability at filtration temperatures employed in the industry of around 700°C, the results will be extrapolated to this temperature in future work.

Introduction

In filtration it is important that particles to be removed contact, or come very close to the filter walls. Therefore the molten metal carrying the inclusions must come into close contact, i.e. wet the filter material. In filtration of aluminium, alumina is the most common filter material, even though alumina is not wetted very well by aluminium [1-3]. Therefore one should investigate the use of alternative filter materials with improved wetting. In the laboratory, SiC and graphite demonstrate good wetting by molten aluminium. Problems with these materials exist, as SiC is easily oxidized to SiO_2 and graphite reacts with Al to give Al_4C_3 .

Once metal has entered the filter, oxidation is not a problem because the solubility of oxygen in aluminium is low, around 1.43×10^{-4} at.% at 700°C [4].

In the molten aluminium/filter environment, the oxygen potential is very low. To study wetting of SiC and graphite in such a system, a high vacuum laboratory furnace containing only a minute amount of oxygen has been chosen.

1.1 Al-SiC System

Wettability of aluminium has been reported for single crystal SiC [5], reaction bonded SiC [6], and sintered SiC [6, 7] (Figure 1). Wettability may change with the preparation process and the sintering aids for SiC. Aluminium has a decreasing contact angle on SiC with increasing temperature. Reaction bonded SiC has better wettability with aluminium than single crystal SiC and sintered SiC. For example, Figure 1 shows that at 830 °C, reaction bonded SiC, single crystal SiC, and sintered SiC have contact angles of 37°, 60°, and 107°, respectively.

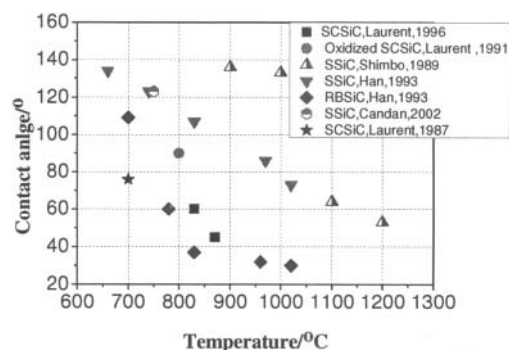


Figure 1 The equilibrium contact angle vs. temperature for aluminium on SiC from literature [5-10]
SSiC- sintered SiC; RBSiC- reaction bonded SiC; SCSiC- single crystal SiC

In aluminium filtration, filters are primed to allow metal to flow through the filter without freezing. The pre-heating temperature is probably up to 1000°C and SiC filter materials will oxidize at this temperature. The oxidation of SiC is very slow at room temperature [11], but SiC will react with air to form a silica-rich surface layer at temperatures above 700 °C in air. SiC oxidation is controlled by the diffusion of oxygen molecules (or oxygen ions) through the thin oxide film [12]. The oxidation behaviour of SiC is also influenced by factors such as moisture, SiC particle size, and metal impurities [12]. In addition to preheating temperature of 1000°C, one should also take into account that the ceramic foam filters (CFF) are “baked” at temperatures above 1000°C. Thus the wettability of oxidized SiC by molten aluminium is important to study in aluminium filtration.

V. Laurent et.al.[8] have shown that silica acts as an oxygen donor to extend the life time of the Al_2O_3 layer on an aluminium drop by the reaction



The reaction between aluminium and SiO_2 does not improve the wetting of aluminium on SiC, shown as the circle marker in Figure 1. The silica layer is changed into alumina and the equilibrium contact angle is the same as aluminium on alumina. With time in high vacuum, a thin initial layer of silica can be removed by reactions (1) and (2) successively.



Aluminium is then in direct contact with SiC and wetting is determined by the Al-SiC system. The role of the silica here is to delay the wetting of aluminium on SiC [8].

Addition of Mg, Ca, Ti and Pb to aluminium enhances the wetting of Al-SiC [10, 13]. For example, the addition of 5 wt% Mg in aluminium results in wetting ($\theta < 90^\circ$) at 700-960°C [6] since Mg reacts with Al_2O_3 and consumes the oxide layer on Al. The addition of Si will not influence wetting [13].

When the liquid composition reaches the peritectic point at 650°C, the following ternary quasi-peritectic reaction [9] occurs isothermally (See Figure 20).



Thus the addition of Si to aluminium prevents the formation of Al_4C_3 and does not affect wettability [9, 14]. The free Si in reaction bonded SiC also prevents the formation of Al_4C_3 [15] and is reported to be effective in promoting wetting by liquid aluminium in the temperature range of 700-1040°C [6]. This may be due to the additional Si-Al bond on the Al-SiC interface and the aluminium penetration into the SiC along the intergranular free silicon resulting from the reaction bonding process in the extensive reaction zone [16].

1.2 Al-Graphite System

Carbon filters have been industrialized as petrol coke filter-DUFI during 1970-1985, known for removing hydrogen, alkaline metals, and non-metallic inclusions in plants operated by ALUSUISEE Group and elsewhere [17]. However Al_4C_3 has a negative effect on the possible use of the graphite as a filter. The Al_4C_3 crystals formed as a reaction product are brittle and highly sensitive to moisture and promote accelerated fatigue crack growth rates due to their hydrophilic nature [18].

The wetting behaviour of the Al-graphite (or Al- Al_4C_3) system will be investigated from the view point of inclusion-metal wettability in filtration.

During the last few decades, several studies had been devoted to the wetting behaviour of the Al-graphite system. As a reactive wetting system, it is agreed that 1) the final or steady contact angle is equal or close to the equilibrium contact angle of the liquid on the reaction product, Al_4C_3 [19]; According to Tomsia et al. [6] in [19], the wetting behaviour of the reaction product is governed by the formation of adsorption layers at the interface, rather than by the subsequent nucleation and growth of the reaction product; 2) wettability would not be improved by the chemical reaction itself. The interatomic force is not correlated to the Gibbs free energy as an exchange of atoms is involved in a chemical reaction [20]. In the Al-graphite system, the final contact angle, θ_2 on the reaction product Al_4C_3 is much lower than the initial contact angle, θ_0 on the original substrate graphite.

Experimental Procedure

The study of the wettability of Al-graphite and Al-SiC by the sessile drop technique gives rise to two main points. The first point is that liquid aluminium reacts with substrates forming Al_4C_3 at and close to the interface, after which the wetting of Al-substrate transforms to the wetting of an Al- Al_4C_3 system. The second point is that liquid aluminium is covered by an oxide layer which inhibits wetting.

Contact angles of liquid aluminium on the substrate were measured using the sessile drop method. The experimental apparatus is schematically shown in [21]. The apparatus essentially consists of a horizontal graphite heater surrounded by

graphite radiation shields, located in a water-cooled vacuum chamber. The chamber was fitted with windows to allow a digital video camera (Sony XCD-SX910CR) to record the shape of the droplet. The contact angles and linear dimensions of the images were measured directly from the image of the drop using the Video Drop Shape Analysis software.

The experiments were carried out using 99.999% pure aluminium and substrates produced from 98.9% single crystal SiC (Washington Mills, Norway) and ISO-88 Graphite substrates. The average roughness of SiC and graphite was 51.25nm and 179.76nm, respectively. The aluminium rod with a diameter of 2mm was cut into small pieces around 2 mm in length, then polished by 500 mesh SiC paper and cleaned with ethanol in order to prevent further oxidation. The SiC single crystal was cut and ground with 1200 mesh diamond paper to get a flat surface, then dried in a closed furnace at 100°C until the experiment was performed in order to minimize the oxidation of the SiC surface.

When the wetting furnace attained the high vacuum of 10^{-5} mbar, the sample was quickly heated to 950°C in about 80s, then heated to 1000, 1100, 1200, and 1300°C at the rate of 50°C/min, as shown in Figure 2. Although the furnace temperature overshoots to 1100°C at the first 80s, it does not affect the wettability at a lower temperature such as 1000°C, since the oxide skin holds the liquid metal at the beginning. In all of the experiments, the contact angle and dimensions of the drop were recorded during the isothermal period at 1000, 1100, 1200, and 1300°C. For the dimension reading, time=0 was taken to be the beginning of the isothermal period.

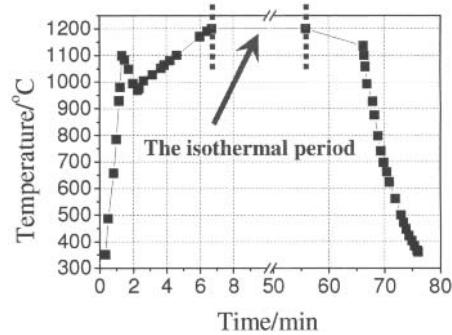


Figure 2 Example of the registered temperature for the experiment holding the sample at 1200 °C

Results

3.1 Al-SiC System

Figure 3 and Figure 4 show the time dependent variations of wetting properties for liquid aluminium on SiC at 1000°C. Three kinetic steps can be distinguished: the first step, where the contact angle decreases rapidly (in 45min) from the initial contact angle $\theta_0 \approx 120^\circ$ to $\theta_1 \approx 81^\circ$; the second step where the contact angle continues to decrease to a relatively low value of $\theta_2 \approx 65^\circ$, but at a slower rate; and the third step where the contact angle stabilized at θ_2 after approximately 150min. The stable base diameter and the sessile volume allow the stable contact angle in the third stage to be measured.

Similar three kinetic steps: (1) rapid decrease, (2) slow decrease and (3) stable contact angle at 1100°C are shown in Figure 5 and Figure 6. The stable base diameter and the sessile volume guarantee the stable contact angle in the third stage. A lower stable contact angle is obtained in a shorter time at 1100°C than at 1000°C (See Table 1).

Efforts to obtain the Al-SiC contact angle at even higher temperatures, for example 1200°C, were made, as shown in Figure 7 and Figure 8. Unfortunately, the evaporation of aluminium at higher temperatures is so high that the aluminium droplet disappeared quickly. The experiment was repeated at a later date

with a larger amount of aluminium and showed good reproducibility (See Figure 7 and Figure 8). Experimental results of aluminium on SiC are summarized in Table 1.

Table 1 Results of aluminium on SiC

Temperature	Step.1	Step.2		Step.3	
	θ_0	θ_1	t_1	θ_2	t_2
1000°C	120°	81°	45min	65°	150min
1100°C	136°	74°	13min	56°	125min

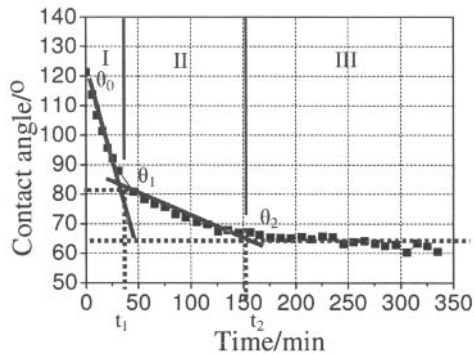


Figure 3 Contact angle vs. time for aluminium on SiC at 1000°C

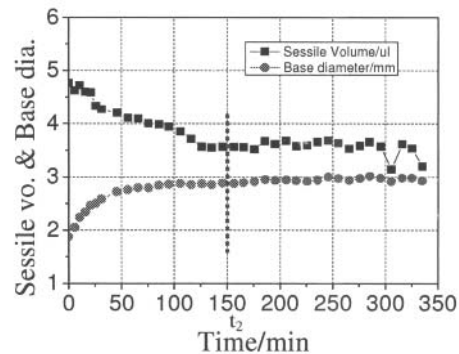


Figure 4 Sessile volume and base diameter vs. time for aluminium on SiC at 1000°C

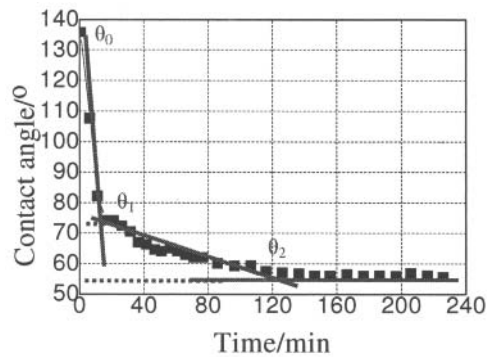


Figure 5 Contact angle vs. time for aluminium on SiC at 1100°C

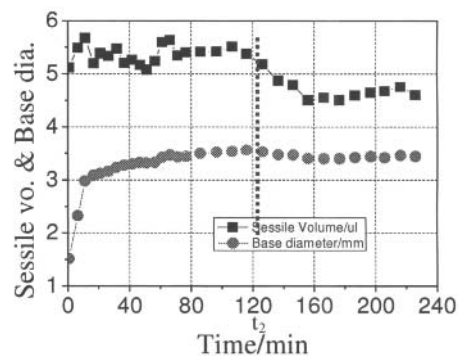


Figure 6 Sessile volume and base diameter vs. time for aluminium on SiC at 1100°C

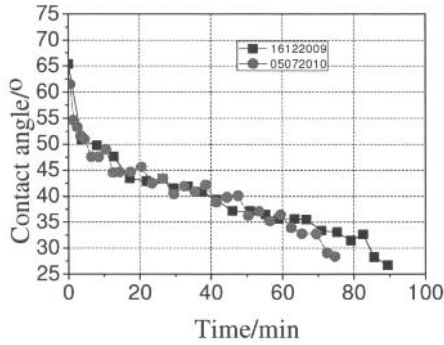


Figure 7 Contact angle vs. time for aluminium on SiC at 1200°C

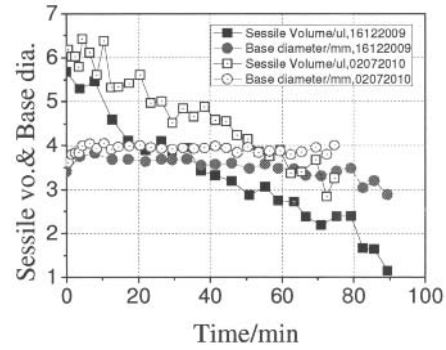


Figure 8 Sessile volume and base diameter vs. time for aluminium on SiC at 1200°C

3.2 Al- Graphite System

Figure 9 and Figure 10 give the wettability between aluminium and graphite at 1000°C as a function of time. The linear decreasing contact angle and the linear increasing base diameter indicate that further holding is required to attain the equilibrium contact angle. The almost constant sessile volume shown in Figure 10 is explained by low evaporation from the aluminium droplet because of its oxide layer.

The wetting properties between aluminium and graphite at 1100°C are shown in Figure 11 and Figure 12. The similar three kinetic steps can be distinguished: the first step, where the contact angle decreases rapidly (in 30min) from the initial contact angle $\theta_0 \approx 157^\circ$ to $\theta_1 \approx 91^\circ$ angle; the second step where the contact angle continues to decrease down to θ_2 but with a slower rate; and the third step corresponding to a nearly constant angle $\theta_2 \approx 65^\circ$ at time 200min. The decreasing sessile volume indicates that de-oxidation of the oxide layer and evaporation from the aluminium drop take place. The stable base diameter and the sessile volume allow the measurement of the stable contact angle in the third stage.

Measurement of the contact angle, sessile drop volume, and base diameter has also been carried out at 1200°C, shown in Figure 13 and Figure 14. Unfortunately, the evaporation of aluminium is high and no stable contact angle was detected.

Experimental results of aluminium on graphite are summarized in Table 2.

Table 2 Results of aluminium on graphite

Temperature	Step.1	Step.2		Step.3	
	θ_0	θ_1	t_1	θ_2	t_2
1000°C	157°		>500min		
1100°C	157°	91°	30min	65°	200min

The initial sessile volumes, 5.6 μl at 1000°C, 5.7 μl at 1100°C, 4.9 μl at 1200°C, and 3.9 μl at 1300°C indicate that evaporation (from the initial heating to the time=0) is almost the same at 1000°C and 1100°C, and evaporation is greater at higher temperatures. The initial base diameters of 0.86mm at 1100°C, 2.2mm at 1200°C, and 3.1mm at 1300°C, as well as decreasing initial contact angles with temperature indicate that better wetting already occurs at the higher temperature before defined time zero.

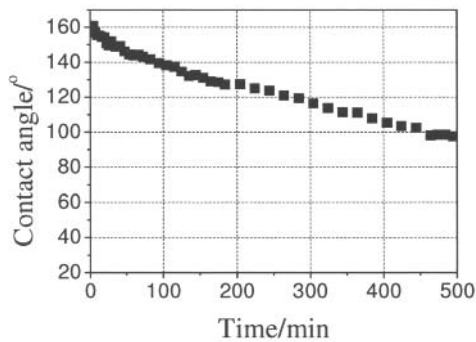


Figure 9 Contact angle vs. time for aluminium on graphite at 1000°C

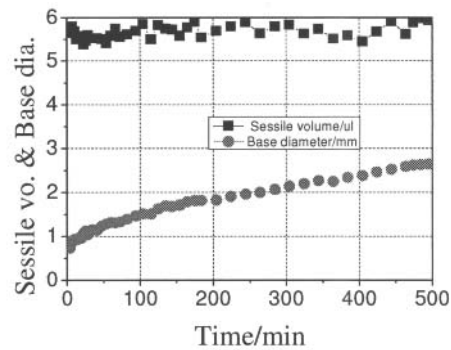


Figure 10 Sessile volume and base diameter vs. time for aluminium on graphite at 1000°C

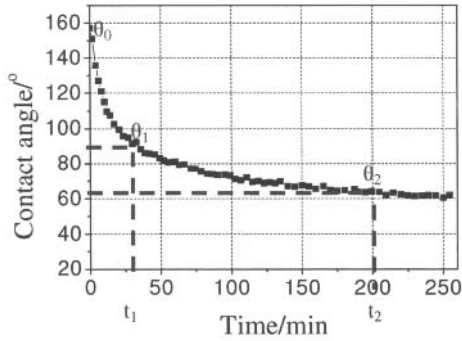


Figure 11 Contact angle vs. time for aluminium on graphite at 1100°C

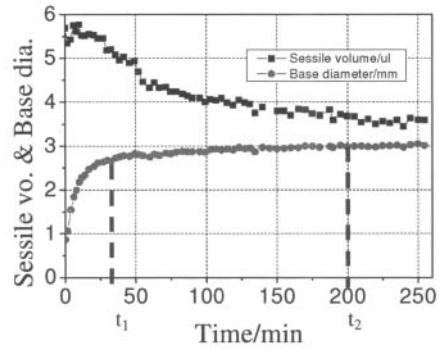


Figure 12 Sessile volume and base diameter vs. time for aluminium on graphite at 1100°C

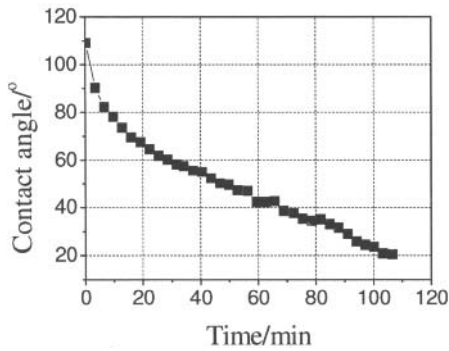


Figure 13 Contact angle vs. time for aluminium on graphite at 1200°C

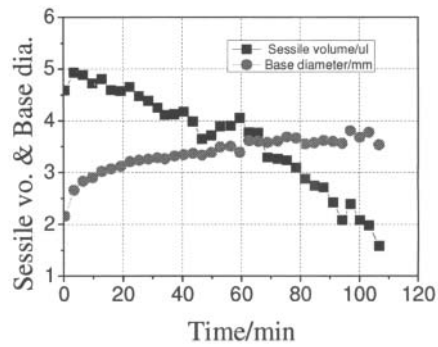


Figure 14 Sessile volume and base diameter vs. time for aluminium on graphite at 1200°C

rate of the aluminium sessile drop volume on SiC and graphite (see Figure 15) supported this assumption.

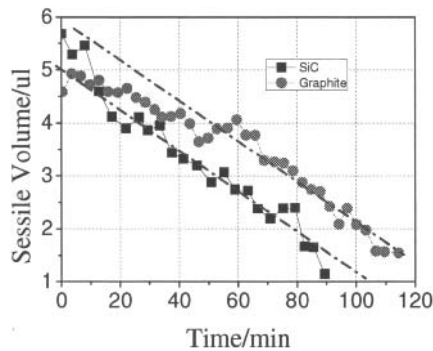


Figure 15 Sessile volume vs. time for aluminium on SiC and graphite at 1200°C



Evaporation in both systems, Al-graphite and Al-SiC, depends only on reactions (2) and (4), independent of the interfacial reaction and the oxidation of the substrate. The same decreasing

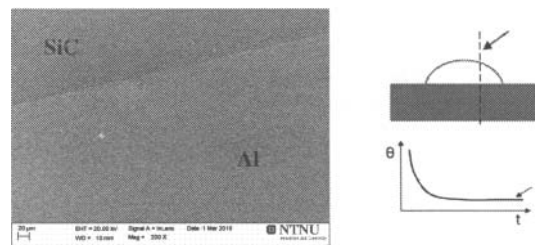


Figure 16 SEM micrograph of a cross section in an Al-SiC specimen cooled naturally after 335 min at 1000°C

On the Al-SiC interface no Al_4C_3 layer was found on the sample cooled in air after 335 min at 1000°C (See Figure 16). However, Figure 17 shows the presence of a continuous layer of a reaction product, Al_4C_3 at the Al-graphite interface with a thickness of 130 μm . The graphite- Al_4C_3 interface is rougher than the graphite substrate before the experiments and pores are present around some particles. Extra aluminium in the Al_4C_3 layer and the discrete Al_4C_3 particles indicates that the reaction proceeds by dissolution of carbon into aluminium. The final contact angle is determined by the Al- Al_4C_3 system.

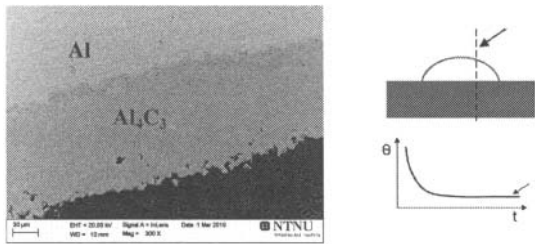


Figure 17 SEM micrograph of a cross section in an Al-graphite specimen cooled naturally after 250 min at 1100°C

Discussion

The three successive steps of wetting kinetics in Figures 3-14 are discussed successively.

Step.1- De-oxidation of oxide layer

The sharp decrease of the contact angle from θ_0 to θ_1 on both Al-SiC and Al-graphite is similar to the contact angle curve observed previously for Al- Al_2O_3 for the same step in the same wetting furnace. This reduction is due to de-oxidation of the oxide layer according to reaction (2). This is effective when the outgoing flow of oxygen in Al_2O (g) is higher than the incoming flow of oxygen. The $P_{\text{Total}}=10^{-3}$ Pa (10^{-5} mbar) in the furnace verifies that $P_{\text{Al}_2\text{O}}$ is lower than the equilibrium $P_{\text{Al}_2\text{O}}=3.7 \times 10^{-3}$ Pa at 1000°C [22]. Thus the wetting behaviour of the first step is controlled by de-oxidation of the oxide layer on the aluminium drop.

Step.2- De-oxidation of silica in the Al-SiC system and the Al_4C_3 formation in the Al-graphite system

There are three possible explanations concerning the second step from θ_1 to θ_2 in Al-SiC system: a) the dissolution of SiC into aluminium according to reaction (5), b) coverage of the interface by Al_4C_3 according to reaction (3), and c) de-oxidation of silica on the interface according to reactions (1) and (2).



The maximum solubility of carbon in liquid aluminium, on the order of 30 ppm at temperatures close to 1000°C [23] is too low to support the dissolution mechanism in a).

The kinetics of the reaction (3) is slow and leads to the limited formation of discrete particles of Al_4C_3 at the interface. Thus the spreading of de-oxidized aluminium is controlled by de-oxidation of SiC with limited amounts of discrete particles of Al_4C_3 . This is supported by the delayed equilibrium contact angle obtained in the Al-oxidized SiC system [8] at 660-900°C.



In the second step from time t_1 to t_2 in Al-graphite system, the spreading velocity is lower than the previous step and the base diameter is a linear function with respect to time. This second step does not exist in the non-reactive Al- Al_2O_3 system [24]. The interfacial reaction (6) has Gibbs energy of -136kJ/mol to -102kJ/mol [25] at temperatures of 660 to 1300°C. Figure 17 also supports that the second step in Al-graphite system is controlled by the formation of Al_4C_3 .

The kinetics of reaction (3) forming Al_3C_4 from SiC is slower than that of reaction (6) forming Al_3C_4 directly, so the stable

contact angle was obtained easily in Al-SiC system with a small amount of Al_4C_3 (See Figure 3 and Figure 9).

Step.3- Stable contact angle

The Al- Al_4C_3 system is formed at the end of the second step in both systems in which a relatively stable contact angle is detected in the third step. Since the liquid droplet and SiC substrate show a strong sensitivity to oxygen, it is not surprising to have the scatter of $\theta_2, \pm 4^\circ$. Good repeatability of wetting properties was observed at the same temperature.

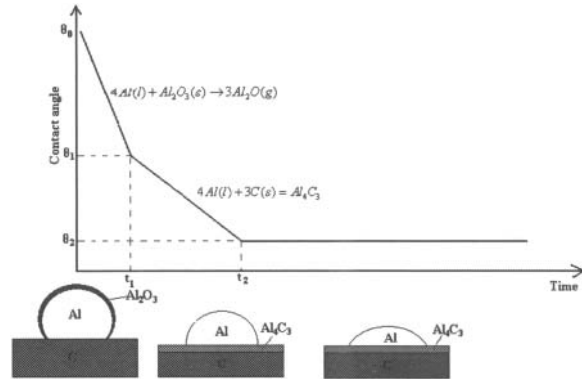


Figure 18 The time dependent wettability of the graphite-Al system

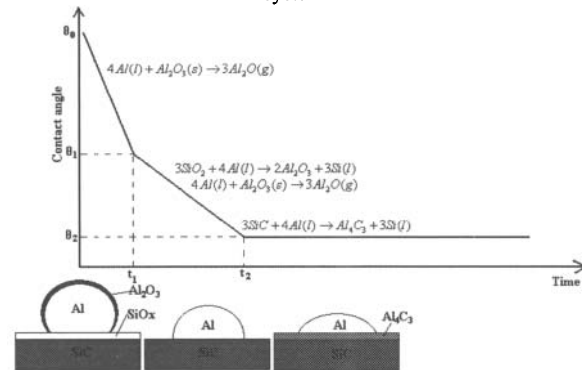


Figure 19 The time dependent wettability of the oxidized SiC-Al system

To summarize the discussion, schematics of the wettability for the Al-SiC and Al-graphite systems are shown in Figure 18 and Figure 19. The contact angle initially changes with time and finally approaches an “equilibrium value”. Both systems produce Al_4C_3 at the end and the interface reaction product promotes the wetting. However, extra silicon in aluminium could prevent the Al_4C_3 formation in Al-SiC system.

Wetting in Filtration

Al_4C_3 inclusions have relatively good wetting with aluminium. Al_4C_3 leads to fatigue cracking in casting and is not easily removed by settling because of its density of 2.36 g/cm³.

The Al-SiC interface properties depend on filtration time. Priming before filtration leads to oxidation of the SiC filter. The silica changes into alumina by reaction (1). Alumina formed by the

reduction of the silica surface likely inhibits nucleation of Al_4C_3 . An aluminium alloy with more than 10% silicon would prevent the Al_4C_3 formation according to reaction (3) (See Figure 20).

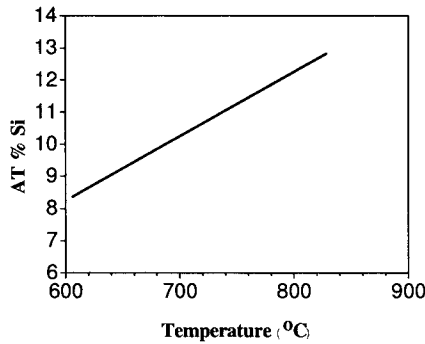


Figure 20 The theoretical silicon level required to prevent Al_4C_3 formation [26]

Conclusions

1. The wettability of Al-SiC and Al-graphite with respect to time can be divided into three kinetic steps: (i) de-oxidation of Al_2O_3 layer, (ii) de-oxidation of silica for Al-SiC system with a small amount of Al_4C_3 (or Al_4C_3 formation for Al-graphite system), and (iii) the stable contact angle.
2. The equilibrium contact angles of the Al-SiC and Al-graphite system under 10^{-8} bar vacuum are shown in Table 3.

Table 3 The equilibrium contact angle

Temperature [°C]	The Al-SiC system		The Al-graphite system	
	[°]	[min]	[°]	[min]
1000	65	150	<97	>500
1100	57	125	65	200

3. Both the SiC filter and Al_4C_3 inclusions have relatively good wetting with aluminium at temperatures greater than $1000^\circ C$.
4. SiC filters are of special interest for the filtration of high Si aluminium alloys.
5. At $700^\circ C$ initially SiC and graphite are poorly wetted by aluminium. Times for wetting to take place may be hours. This will be discussed in future work.

Future Work

The time dependent wetting properties of Al-graphite and SiC at $700^\circ C$ will be extrapolated from the high temperature data. Pilot trials will be carried out in industry to investigate the effect of wettability on filtration efficiency.

Acknowledgment

The authors acknowledge the financial support from RIRA project by the research council of Norway. Thanks are also given to Don Doutré for a fruitful discussion and for providing Figure 20.

References

1. Laurent, V., et al., *Wettability of Monocrystalline Alumina by Aluminium between Its Melting Point and 1273K*. Acta Metallurgica et Materialia, 1988. **36**(7): p. 1797-1803.
2. Klinter, A.J., G. Mendoza-Suarez, and R. A.L.Drew, *Wetting of pure aluminium and selected alloys on polycrystalline alumina and sapphire*. Materials Science and Engineering A, 2008.
3. M.Ksiazek, et al., *Wetting and Bonding Strength in Al/ Al_2O_3 System*. Materials Science and Engineering, 2002. **A324**: p. 162-167.
4. Tang, K., *Wettability of Al on Al_2O_3* . SINTEF report, 2009: p. 6.
5. Laurent, V., C. Rado, and N. Eustathopoulos, *Wetting Kinetics and Bonding of Al and Al Alloys on α -SiC*. Materials Science & Engineering A, 1996. **205**: p. 1-8.
6. Han, D.S., H. Jones, and H.V. Atkinson, *The wettability of silicon carbide by liquid aluminium: the effect of free silicon in the carbide and of magnesium, silicon and copper alloy additions to the aluminium*. Journal of Materials Science, 1993. **28**(10): p. 2654-2658.
7. Shimbo, M.N., M. and I. Okamoto, *Wettability of silicon carbide by aluminum, copper and silver*. Journal of Materials Science Letters, 1989. **8**(6): p. 663-666.
8. Laurent, V., D. Chatain, and N. Eustathopoulos, *Wettability of SiO_2 and oxidized SiC by aluminium*. Materials Science & Engineering A: Structural Materials: Properties, Microstructure and Processing, 1991. **135**(1-2): p. 89-94.
9. Laurent, V., D. Chatain, and N. Eustathopoulos, *Wettability of SiC by aluminium and Al-Si alloys* Journal of Materials Science, 1987. **22**(1): p. 244-250.
10. CANDAN, E., *Effect of Alloying Elements to Aluminium on the Wettability of Al/SiC system*. Turkish J. Eng. Env. Sci., 2002. **26**: p. 1-5.
11. Guy Ervin, J., *Oxidation Behavior of Silicon Carbide*. Journal of the American Ceramic Society, 1958. **41**(9): p. 347-352.
12. Quanli, J., et al., *Effect of particle size on oxidation of silicon carbide powders*. Ceramics International, 2007. **33**: p. 309-313.
13. Moraes, E.E.S., M.L.A. Graça, and C.A.A. Cairo, *Study of Aluminium Alloys Wettability on SiC Preform*. Congresso Brasileiro de Engenharia e Ciência dos Materiais, 2006. **15**(19): p. 4217-4224.
14. Li, J.G., *Wetting of ceramic materials by liquid silicon, aluminium and metallic melts containing titanium and other reactive elements: a review*. Ceramics international, 1994. **20**: p. 391-412.
15. Iseki, T., T. Kameda, and T. Maruyama, *Interfacial reactions between SiC and aluminium during joining*. Journal of Materials Science, 1984. **19**: p. 1692-1698.
16. Foister, S.A.M., M.W. Johnston, and J.A. Little, *The interaction of liquid aluminium with silicon carbide and nitride-based ceramics*. Journal of Materials Science Letters, 1993. **12**(4): p. 209-211.
17. Bornand, J.-D. and K. Buxmann, *DUFI: A Concept of Metal Filtration*. Light Metals, 1985: p. 1249-1260.
18. Etter, T., et al., *Aluminium carbide formation in interpenetrating graphite/aluminium composites*. Materials Science and Engineering A, 2007. **448**(1-6).

19. Kalogeropoulou, S., C. Rado, and N. Eustathopoulos, *Mechanisms of reactive wetting: the wetting to non-wetting case*. Scripta Materialia, 1999. **41**(7): p. 723-728.
20. Zhou, X.B. and J.T.M.D. Hosson, *Reactive wetting of liquid metals on ceramic substrates*. Acta Materialia, 1996. **44**(2): p. 421-426.
21. Bao, S., et al., *Wetting of Pure Aluminium on Filter Materials Graphite, AlF₃ and Al₂O₃*. Light Metals:138th TMS Annual Meeting and Exhibition, Moscone West Convention Center, Feb. , San Francisco, CA, USA, 2009: p. 767-773.
22. Standards, N.B.o., *JANAF Thermochemical Tables, 2nd edition*. 1971. **37**.
23. Yokokawa, H., et al., *Phase relations associated with the aluminium blast furnace. Aluminium oxycarbide metals and Al-C-X (X=Fe, Si) liquid alloys*. Metallurgical Transactions B, 1987. **18B**: p. 433-444.
24. Bao, S., et al., *Wettability of Aluminium on Alumina*. To be published.
25. Isaikin, A.S., et al., *Compatibility of Carbon Filaments with A Carbide Coating and an Aluminium Matrix*. Sci. Heat Treatment, 1980. **22**: p. 815-817.
26. Lloyd, D.J., *The solidification microstructure of particulate reinforced aluminium/SiC composites*. Composites Science and Technology, 1989. **35**: p. 159-179.